

# Right Ventricular Strain Improves Cardiac MRI–based Prognostication in Heart Failure with Preserved Ejection Fraction



Leyi Zhu, PhD<sup>\*1</sup> • Huaying Zhang, PhD<sup>\*1</sup> • Mengdi Jiang, MD<sup>1</sup> • Jing Xu, MD<sup>1</sup> • Di Zhou, MD<sup>1</sup> • Weichun Wu, MD<sup>2,3</sup> • Wenjing Yang, PhD<sup>1</sup> • Yining Wang, PhD<sup>1</sup> • Gang Yin, BS<sup>1,3</sup> • Arlene Sirajuddin, MD<sup>4</sup> • Andrew E. Arai, MD<sup>4,5</sup> • Qiang Zhang, PhD<sup>6</sup> • Shihua Zhao, MD, PhD<sup>\*\*1</sup> • Minjie Lu, MD, PhD<sup>\*\*1,3</sup>

<sup>\*</sup> L.Z. and H.Z. contributed equally to this work.

<sup>\*\*</sup> S.Z. and M.L. are co–senior authors.

Author affiliations, funding, and conflicts of interest are listed at the end of this article.

See also the editorial by Murphy and Quinn in this issue.

Radiology 2025; 315(3):e243080 • <https://doi.org/10.1148/radiol.243080> • Content codes:  

**Background:** Right ventricular (RV) function is an independent predictor of clinical status and prognosis in multiple cardiovascular diseases; however, the prognostic value of RV strain in patients with heart failure with preserved ejection fraction (HFpEF) remains largely unknown.

**Purpose:** To determine the associations between RV strain variables derived from cardiac MRI feature tracking and adverse outcomes in patients with HFpEF.

**Materials and Methods:** This retrospective study included patients with HFpEF who underwent cardiac MRI from January 2010 to December 2018. The primary end point was all-cause mortality. The results were validated in a cohort of patients with HFpEF enrolled from January 2019 to June 2021. Cox regression analysis was performed to assess the associations between variables and clinical outcomes.

**Results:** The development cohort comprised 1019 patients (mean age, 56.9 years  $\pm$  12.3 [SD]; 710 men), and the validation cohort comprised 273 patients (mean age, 55.3 years  $\pm$  14.0; 191 men). During a median follow-up of 7.8 and 3.9 years, respectively, 103 patients in the development cohort and nine in the validation cohort died. Multivariable Cox regression analysis showed that RV global longitudinal and circumferential strain were independent predictors of all-cause mortality (adjusted hazard ratio per 1% increase, 1.07 [95% CI: 1.02, 1.12;  $P$  = .005] and 1.13 [95% CI: 1.05, 1.21;  $P$  < .001], respectively). The full model based on clinical, conventional imaging, and RV strain variables demonstrated the best discrimination performance in the development (C index = 0.794) and validation (C index = 0.782) cohorts. In a subgroup with T1 mapping data, RV global longitudinal and circumferential strain remained independent predictors after separate adjustment for native T1 value and extracellular volume fraction (all models,  $P$  < .05).

**Conclusion:** RV global longitudinal and circumferential strain derived from cardiac MRI were independent predictors of adverse outcomes in patients with HFpEF, providing greater prognostic value than traditional clinical and imaging-derived risk markers.

© RSNA, 2025

Supplemental material is available for this article.

Heart failure (HF) with preserved ejection fraction (HFpEF) accounts for more than half of all HF cases and presents a unique medical challenge because of its complex pathophysiologic characteristics and heterogeneity in clinical presentation and outcomes (1,2). While left ventricular (LV) function has been extensively studied and used as a prognostic tool in patients with HFpEF, right ventricular (RV) dysfunction is increasingly being recognized as a crucial determinant of clinical outcomes (3–5).

The LV and RV have close interactions and are intricately coordinated. The elevated LV filling pressure that occurs in HFpEF leads to an increase in left atrial (LA) filling pressure, consequently increasing RV afterload (6). This could be the primary mechanism of RV dysfunction in patients with HFpEF given that the RV chamber is more sensitive to changes in afterload (7). LV and RV function are also anatomically interrelated due to the continuity of myocardial fibers and the interventricular septum. Despite the preserved LV ejection fraction in patients with HFpEF, there are still subtle impairments in LV systolic function (8), which in turn contribute to RV dysfunction.

Recently, myocardial strain parameters derived from speckle-tracking echocardiography and cardiac MRI feature tracking (FT) have shown potential in assessing myocardial deformation and detecting early or subclinical abnormalities in systolic and diastolic function (9). LV global longitudinal strain (GLS) has been established as a strong prognostic marker in patients with HFpEF (10,11); however, few studies have focused on the prognostic implications of RV dysfunction as evaluated using myocardial strain analysis. Some echocardiographic studies have indicated that an RV strain metric derived from speckle tracking is an independent predictor of adverse outcomes in patients with HFpEF (12,13). Nevertheless, echocardiography is highly dependent on adequate acoustic windows; thus, the acquisition is especially challenging in patients with HFpEF, who often have comorbid obesity or chronic obstructive pulmonary disease. The thinness and complex shape of the RV wall, and its location behind the sternum, pose additional obstacles to assessing RV function using echocardiography (14). Cardiac MRI is the standard for noninvasive assessment of cardiac structure and function. The European Society of Cardiology recommends cardiac MRI as the

## Abbreviations

FT = feature tracking, GCS = global circumferential strain, GLS = global longitudinal strain, HF = heart failure, HFpEF = HF with preserved ejection fraction, HR = hazard ratio, LA = left atrium, LV = left ventricle, RV = right ventricle, RVEF = RV ejection fraction

## Summary

Right ventricular global longitudinal and circumferential strain derived from cardiac MRI were independently associated with adverse outcomes in a large cohort of patients with heart failure with preserved ejection fraction.

## Key Results

- In a retrospective cohort study of 1019 patients with heart failure with preserved ejection fraction, right ventricular (RV) global longitudinal and circumferential strain derived from cardiac MRI feature tracking were associated with all-cause mortality (adjusted hazard ratio per 1% increase, 1.07 [ $P = .005$ ] and 1.13 [ $P < .001$ ], respectively).
- The model combining clinical, conventional imaging, and RV strain variables exhibited the best model discrimination for all-cause mortality (C index = 0.794).
- Even after adjustment for tissue characterization data, RV global longitudinal and circumferential strain remained independent predictors of all-cause mortality (all models,  $P < .05$ ).

best alternative imaging modality for patients with HFpEF with nondiagnostic echocardiographic examinations, especially for right-sided heart evaluation (15). However, limited data are available on the prognostic value of RV function assessed with cardiac MRI FT in patients with HFpEF. Therefore, the aim of this study was to evaluate the associations between RV strain variables derived from cardiac MRI FT and adverse clinical outcomes in patients with HFpEF.

## Materials and Methods

### Study Population

This retrospective study was approved by the institutional ethics review board of Fuwai Hospital (approval no. 2019-1307). Consecutive patients with suspected HFpEF who underwent echocardiography and cardiac MRI at Fuwai Hospital from January 2010 to December 2018 were retrospectively enrolled. These patients constituted the development cohort for the prognostic models. The diagnosis of HFpEF was based on European Society of Cardiology guidelines from 2016 (15) and 2019 (16), as described previously (17). Detailed inclusion and exclusion criteria are provided in Appendix S1. A validation cohort of patients with HFpEF presenting at Fuwai Hospital from January 2019 to June 2021 who met the same inclusion and exclusion criteria as the original development cohort was also enrolled. Baseline clinical data were collected from electronic medical records.

### Echocardiographic Protocol and Analysis

All patients underwent echocardiographic examinations using Philips (EPIQ 7 or iE33) or General Electric (Vivid E9) devices. The digitally stored images were analyzed offline by two radiologists (W.W. and M.L., both with more than 15 years of experience) who were blinded to the clinical data. The analysis details are presented in Appendix S1.

### Cardiac MRI Protocol and Analysis

A standardized cardiac MRI protocol with retrospective electrocardiogram gating and eight-channel cardiac coils was performed (18). Of the patients in the original development cohort, 66.1% (674 of 1019) were examined using a 1.5-T system (Magnetom Avanto; Siemens Healthineers), and 33.9% (345 of 1019) were examined using a 3.0-T system (Ingenia [Philips] or MR750 [General Electric]). All patients in the validation cohort were examined using a 3.0-T system (Ingenia [Philips], MR750 [General Electric], or Magnetom Skyra [Siemens Healthineers]). A standard steady-state free precession cine sequence was used to acquire cine images in the long-axis view (two-, three-, and four-chamber) and consecutive short-axis views. Further information on the standardized cardiac MRI protocol and postprocessing is available in Appendix S1.

RV, LV, and LA strain analyses were performed using the FT technique implemented in cvi42 software (Circle Cardiovascular Imaging), as illustrated in Figure 1. For RV and LV strain analysis, three-directional strain parameters were acquired: GLS, global circumferential strain (GCS), and global radial strain. LV GLS was derived from two-, three-, and four-chamber views, whereas RV GLS was derived from only the four-chamber view. The GCS and global radial strain of the LV and RV walls were calculated from a stack of short-axis views. Papillary muscles were excluded from the endocardial contour (19). For LA strain analysis, LA epicardial and endocardial contours were outlined on two-, three-, and four-chamber views to obtain three-phase strain parameters: reservoir, conduit, and booster strain. The LA appendage and pulmonary veins were excluded from the LA endocardial contours (20). Details on the reproducibility analysis are provided in Appendix S1.

### Follow-up and Clinical Outcomes

The primary end point was all-cause death, and the secondary end point was cardiovascular death (HF death, fatal myocardial infarction, sudden death, stroke, or cardiovascular hemorrhage, according to standardized definitions) (12,21). End points were determined using hospital records, clinic visits, and telephone calls. Telephone interviews were conducted with patients who had missed regular hospital appointments (or their relatives) to obtain their medical records and ascertain if end points had occurred. All suspected events were independently reviewed by two authors (L.Z. and H.Z.) who were blinded to cardiac MRI and postprocessing results.

### Statistical Analysis

Variables are presented as means with SDs, medians with IQRs, or frequencies with percentages, as appropriate. Between-group differences in continuous variables were evaluated using the Student  $t$  test or the Mann-Whitney  $U$  test, and differences in categorical variables were evaluated using the  $\chi^2$  test. Multiple imputation with chained equations, or MICE, with the predictive mean matching method was performed to address missing data (<20% per variable) for laboratory findings. The associations between myocardial strain and conventional cardiac MRI variables were evaluated using the Pearson correlation method. Intra- and interobserver variability was analyzed using intra- and interclass correlation coefficients.

Univariable and multivariable Cox regression analyses were used to investigate the associations between variables and clinical

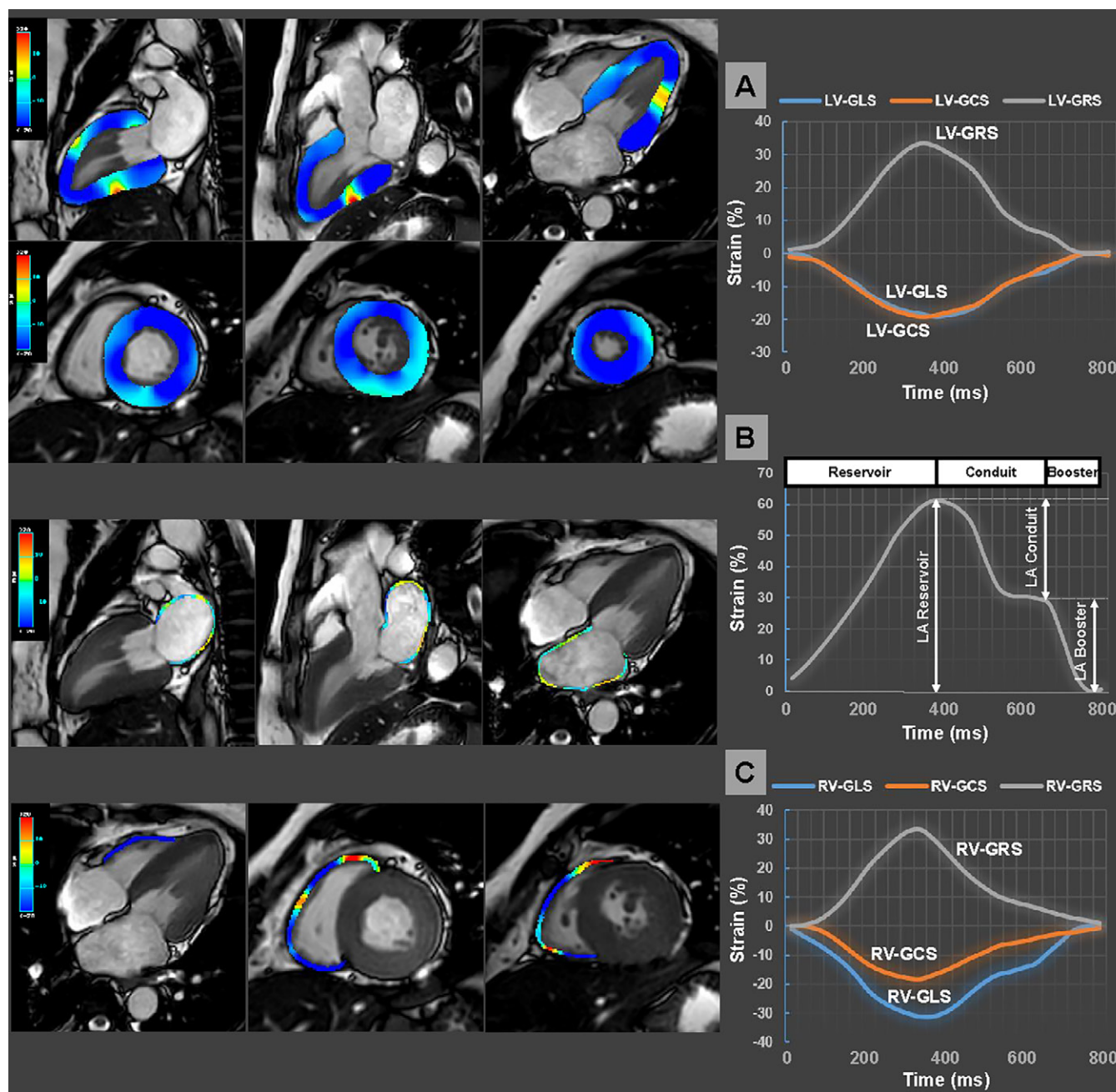


**Figure 1:** Example of left ventricular (LV), left atrial (LA), and right ventricular (RV) strain analysis based on cardiac MRI feature tracking in a 45-year-old male patient with heart failure with preserved ejection fraction. **(A)** Representative plot of LV strain parameters (right), including LV global longitudinal strain (GLS), LV global circumferential strain (GCS), and LV global radial strain (GRS), calculated from cine images in the two-, three-, and four-chamber views (left, first row) and a stack of short-axis views (left, second row). **(B)** Representative plot of LA strain parameters (right), including LA reservoir, conduit, and booster strain, calculated from cine images in the two-, three-, and four-chamber views (left). **(C)** Representative plot of RV strain parameters (right), including RV GLS, RV GCS, and RV GRS, calculated from cine images in the four-chamber view and a short-axis stack (left).

outcomes. Hazard ratios (HRs) with 95% CIs were calculated. Variables with  $P < .05$  in the univariable analysis were included in the multivariable analysis using a stepwise forward selection method. The method for variable selection is detailed in Appendix S1. The contribution of each predictor in the full model was calculated as its partial  $\chi^2$  statistic minus the degrees of freedom (22). Unadjusted survival curves were plotted using the Kaplan-Meier method, and adjusted survival curves were derived from the Cox regression model. The incremental prognostic values of strain variables were evaluated by considering model discrimination, as indicated by the Harrell C index, and model calibration, as indicated by the  $\chi^2$  test, for models with variables incrementally

added. The performance of each model was evaluated by applying the intercept and regression coefficients obtained in the original development cohort to both 10-fold cross-validation and the validation cohort to calculate the Harrell C index (23). Time-dependent receiver operating characteristic analysis was performed to assess the prediction accuracy of each model. Areas under the curve were compared using the DeLong test, and  $P$  values were adjusted for multiple comparisons using Bonferroni correction. To validate the prognostic value of RV strain variables independent of T1 mapping data, a subgroup analysis adjusting for native T1 value and extracellular volume fraction was conducted using multivariable Cox regression analysis.



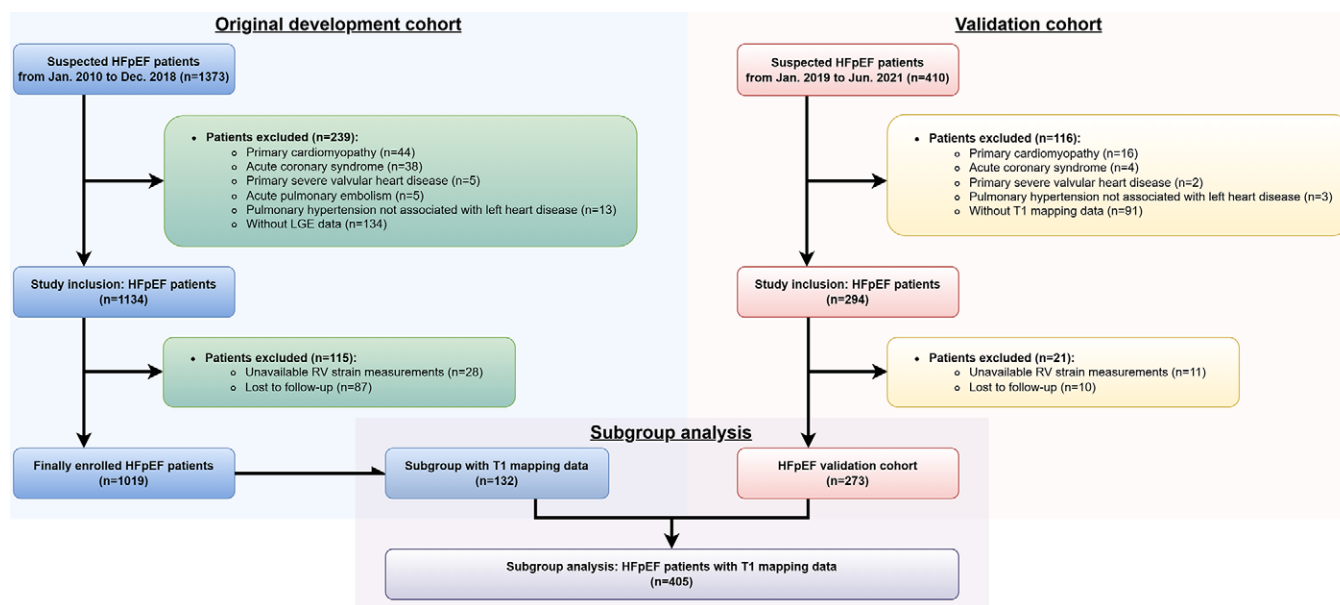


**Figure 2:** Study flowchart. HFpEF = heart failure with preserved ejection fraction, LGE = late gadolinium enhancement, RV = right ventricle.

Differences were considered statistically significant with two-sided  $P < .05$ . All analyses were performed using SPSS (version 27.0; IBM) and R (version 4.3.2; R Foundation for Statistical Computing).

## Results

### Patient Characteristics

A total of 1019 patients (mean age,  $56.9 \text{ years} \pm 12.3 \text{ [SD]}$ ; 710 [70%] male patients) were included in the original development cohort (Fig 2). Most patients (839 of 1019; 82%) were classified as having New York Heart Association class II HF. Nearly all patients (1011 of 1019; 99%) exhibited LV diastolic dysfunction at echocardiography (Table 1). The median LV ejection fraction and the mean RV ejection fraction (RVEF) from cardiac MRI were 55.6% (IQR, 51.6%–62.0%) and  $51.2\% \pm 10.1$ , respectively (Table 2). RV strain variables showed moderate correlations with RVEF ( $|r| = 0.34\text{--}0.42$ ; all  $P < .001$ ) (Fig S1). The validation cohort comprised 273 patients with HFpEF (mean age,  $55.3 \text{ years} \pm 14.0$ ; 191 [70%] male patients) (Fig 2). The baseline characteristics of patients in the validation cohort are summarized in Table S1.

During a median follow-up of 7.8 years (IQR, 5.9–10.2 years), 103 (10.1%) patients died of any cause (primary end point), and 80 (7.9%) patients died with a cardiovascular cause of death (secondary end point) (HF death: 65 of 1019 [6.4%]; fatal myocardial infarction: four [0.4%]; sudden death: eight [0.8%]; stroke: two [0.2%]; cardiovascular hemorrhage: one [0.1%]). Patients who died of any cause showed greater impairment of LV GLS than patients who did not die (mean LV GLS,  $-12.8\%$  vs  $-14.0\%$ ). The impairments in RV GLS (mean,  $-19.4\%$  vs  $-21.8\%$ ), RV GCS (mean,  $-12.4\%$  vs  $-13.6\%$ ), and RV global radial strain (mean,  $19.6\%$  vs  $22.2\%$ ) were also greater in patients who died. Representative LV and RV strain measurements in two patients with HFpEF—one who died and one who did not—are shown in Figure 3.

### Correlations between Cardiac MRI Variables and Clinical Outcomes

Univariable Cox regression analysis revealed that all LV, LA, and RV strain variables were associated with the primary end point (all  $P < .05$ ) (Table 3). RV GLS and RV GCS remained independent predictors of the primary end point (adjusted HR per 1% increase, 1.07 [95% CI: 1.02, 1.12;  $P = .005$ ] and 1.13 [95% CI: 1.05, 1.21;  $P < .001$ ], respectively) in the multivariable analysis, as did age, estimated glomerular filtration rate, LA maximum volume index, and presence of late gadolinium enhancement. LV GLS and RVEF did not remain significant predictors in the multivariable analysis (both  $P > .05$ ). Figure S2 illustrates the relative importance of each variable selected in the multivariable analysis to be part of the full model. Following age, RV GCS was the second most important prognostic marker in the full model, with late gadolinium enhancement ranking third and RV GLS ranking fifth. Survival curves showed that patients with impaired RV strain (RV GLS or RV GCS lower than the median value [ $-21.8\%$  and  $-13.5\%$ , respectively]) and late gadolinium enhancement had poorer outcomes than those with normal RV strain, with and without adjustment for age, estimated glomerular filtration rate, and LA maximum volume index (unadjusted HR, 4.88 [95% CI: 2.68, 8.89;  $P < .001$ ]; adjusted HR, 4.53 [95% CI: 2.48, 8.29;  $P < .001$ ]) (Fig 4).

RV GLS and RV GCS were also independent predictors of the secondary end point (adjusted HR per 1% increase, 1.08 [95% CI: 1.03, 1.14;  $P = .003$ ] and 1.14 [95% CI: 1.06, 1.24;  $P = .001$ ], respectively) after adjustment for clinical and conventional cardiac MRI variables, including age, LV end-diastolic mass index, LA maximum volume index, and presence of late gadolinium enhancement. Again, LV GLS and RVEF were not independent predictors of the secondary end point (both  $P > .05$ ) (Table S2).

Given the use of scanners from multiple vendors and with different field strengths, a sensitivity analysis was performed, which revealed that RV GLS and RV GCS remained independent

**Table 1: Baseline Characteristics of the Study Population**

Characteristic	All Patients ( <i>n</i> = 1019)	Patients Who Survived ( <i>n</i> = 916)	Patients Who Died (Primary End Point) ( <i>n</i> = 103)
Mean age (y)	56.9 ± 12.3	56.0 ± 11.9	65.1 ± 12.3
Median age (y)	57 (49–66)	56 (48–65)	67 (59–74)
Age range (y)	18–89	18–84	27–89
Sex			
Male	710 (70)	647 (71)	63 (61)
Female	309 (30)	269 (29)	40 (39)
Body mass index*	26.4 ± 4.0	26.5 ± 3.8	25.1 ± 4.8
Systolic blood pressure (mm Hg)	133.5 ± 20.1	133.2 ± 19.7	136.2 ± 23.0
Heart failure NYHA class			
II	839 (82)	763 (83)	76 (74)
III	159 (16)	136 (15)	23 (22)
IV	21 (2)	17 (2)	4 (4)
Smoking	416/974 (43)	369/871 (42)	47/103 (46)
Comorbidities			
Hypertension	778 (76)	694 (76)	84 (82)
Coronary artery disease	371 (36)	322 (35)	49 (48)
Diabetes	281 (28)	244 (27)	37 (36)
Atrial fibrillation	333 (33)	297 (32)	36 (35)
Medication			
ACEI or ARB	575/1006 (57)	519/904 (57)	56/102 (55)
β-blocker	731/1006 (73)	658/904 (73)	73/102 (72)
Calcium channel blocker	370/1006 (37)	330/904 (37)	40/102 (39)
Diuretic	381/1006 (38)	325/904 (36)	56/102 (54)
Aspirin	584/1006 (58)	516/904 (57)	68/102 (67)
Statin	466/1006 (46)	414/904 (46)	52/102 (51)
Amiodarone	81/1006 (8)	73/904 (8)	8/102 (8)
Laboratory findings			
eGFR (mL/min/1.73 m <sup>2</sup> , <i>n</i> = 950) <sup>†</sup>	84.5 ± 18.9	85.7 ± 18.4	74.4 ± 19.7
NT-proBNP (pg/mL, <i>n</i> = 847) <sup>†</sup>	282.8 (176.8–580.0)	272.8 (172.3–563.6)	486.4 (274.4–922.6)
Echocardiographic parameters			
LV relative wall thickness (%)	41.3 ± 9.3	41.2 ± 9.2	42.0 ± 10.7
LA anteroposterior diameter (mm)	39.4 ± 6.1	39.3 ± 6.0	40.8 ± 6.9
E (cm/sec)	81.4 ± 24.3	81.0 ± 23.8	84.2 ± 28.1
E/A < 1 or E/e' > 13	1011 (99)	908 (99)	103 (100)
TRV (m/sec; <i>n</i> = 375)	2.6 ± 0.4	2.6 ± 0.4	2.7 ± 0.6

Note.—Continuous data are reported as means ± SDs or medians with IQRs in parentheses. Categorical data are reported as numbers of patients with percentages in parentheses. A = late diastolic mitral inflow velocity, ACEI = angiotensin-converting enzyme inhibitor, ARB = angiotensin receptor blocker, E = early diastolic mitral inflow velocity, e' = mean mitral annular peak early diastolic velocity, eGFR = estimated glomerular filtration rate, LA = left atrium, LV = left ventricle, NT-proBNP = N-terminal fragment of the prohormone of brain natriuretic peptide, NYHA = New York Heart Association, TRV = tricuspid regurgitation velocity.

\* Calculated as weight in kilograms divided by height in meters squared.

<sup>†</sup> Before multiple imputation.

predictors of both end points after adjustment for scanner vendor and field strength (all *P* < .001) (Table S3).

### Prognostic Value of Cardiac MRI Metrics in Risk Stratification Models

To evaluate the incremental prognostic value of cardiac MRI–derived metrics beyond clinical variables, four models were constructed to predict the primary end point. The full model (model 4), based on clinical, conventional imaging, and RV strain variables, showed improved discrimination ability (C index = 0.794) compared with model 1, which was based solely on clinical variables (C index = 0.716), and model 3, which incorporated

clinical and conventional imaging variables (C index = 0.760). Model 4 also showed better model calibration than model 1 and model 3 (both *P* < .001), with a  $\chi^2$  value of 126.90 (Table 4). Furthermore, the addition of RV strain to predefined models based on LV GLS, LA strain variables, and RVEF yielded further improvements in model discrimination and calibration (Table S4). Similar results were observed in the time-dependent receiver operating characteristic analysis over the entire follow-up period, with model 4 showing the highest prediction accuracy (overall area under the curve, 0.803) (Fig 5).

Similarly, four models were constructed to predict the secondary end point. The full model (model D), which incorporated

**Table 2: Baseline Cardiac MRI Data of the Study Population**

Variable	All Patients (n = 1019)	Patients Who Survived (n = 916)	Patients Who Died (Primary End Point) (n = 103)
<b>Conventional cardiac MRI variables</b>			
LVEF (%)	55.6 (51.6–62.0)	56.0 (51.6–62.2)	53.2 (50.7–59.2)
LV wall thickness (mm)	12.0 ± 3.4	12.0 ± 3.3	12.4 ± 4.0
LVEDVi (mL/m <sup>2</sup> )	78.1 ± 21.8	77.7 ± 21.0	81.8 ± 27.2
LVESVi (mL/m <sup>2</sup> )	33.8 ± 12.2	33.5 ± 11.8	36.9 ± 15.1
LVMi (g/m <sup>2</sup> )	58.2 ± 19.4	57.9 ± 19.0	60.7 ± 22.2
LAEF (%)	43.7 ± 14.3	44.2 ± 13.9	39.3 ± 16.5
LAVi max (mL/m <sup>2</sup> )	49.4 ± 22.9	48.4 ± 22.4	58.7 ± 25.1
LAVi min (mL/m <sup>2</sup> )	29.8 ± 20.6	28.7 ± 20.1	39.3 ± 22.7
RVEF (%)	51.2 ± 10.1	51.4 ± 9.8	49.0 ± 11.7
RVEDVi (mL/m <sup>2</sup> )	75.1 ± 19.8	75.3 ± 19.6	73.6 ± 21.9
RVESVi (mL/m <sup>2</sup> )	36.7 ± 12.4	36.6 ± 12.1	37.6 ± 14.9
Presence of LGE	339 (33)	285 (31)	54 (52)
Ischemic LGE	183 (18)	150 (16)	33 (32)
Nonischemic LGE	170 (17)	146 (16)	24 (23)
LGE mass (g)	3.2 ± 7.2	3.0 ± 7.0	5.6 ± 8.5
LGE percentage of LV mass (%)	2.9 ± 6.3	2.7 ± 6.0	5.1 ± 7.6
<b>Cardiac MRI–derived strain variables</b>			
LV GLS (%)	−13.9 ± 3.4	−14.0 ± 3.4	−12.8 ± 3.5
LV GCS (%)	−16.4 ± 3.4	−16.5 ± 3.4	−15.8 ± 3.3
LV GRS (%)	27.1 ± 8.1	27.3 ± 8.1	25.5 ± 8.0
LA reservoir strain (%)*	32.8 ± 11.5	33.4 ± 11.3	26.7 ± 11.6
LA conduit strain (%)*	15.0 ± 7.1	15.4 ± 7.1	11.1 ± 6.2
LA booster strain (%)*	17.7 ± 6.6	17.9 ± 6.5	15.6 ± 7.3
RV GLS (%)	−21.6 ± 4.5	−21.8 ± 4.5	−19.4 ± 4.3
RV GCS (%)	−13.5 ± 2.9	−13.6 ± 2.8	−12.4 ± 3.1
RV GRS (%)	21.9 ± 6.4	22.2 ± 6.3	19.6 ± 6.2

Note.—Continuous data are reported as means ± SDs or medians with IQRs in parentheses. Categorical data are reported as numbers of patients with percentages in parentheses. GCS = global circumferential strain, GLS = global longitudinal strain, GRS = global radial strain, LA = left atrium, LAEF = LA ejection fraction, LAVi max = LA maximum volume index, LAVi min = LA minimum volume index, LGE = late gadolinium enhancement, LV = left ventricle, LVEDVi = LV end-diastolic volume index, LVEF = LV ejection fraction, LVESVi = LV end-systolic volume index, LVMi = LV end-diastolic mass index, RV = right ventricle, RVEDVi = RV end-diastolic volume index, RVEF = RV ejection fraction, RVESVi = RV end-systolic volume index.

\* LA reservoir, conduit, and booster strain data were available for 745 patients.

clinical, conventional imaging, and RV strain variables, had the highest C index (0.827), higher than that of model A, which was based solely on clinical variables (C index = 0.701), and model C, which was based on clinical and conventional imaging variables (C index = 0.789). Model D showed similar improvements in model calibration compared with model A and model C (both  $P < .001$ ). Integrating RV strain into predefined models based on LV GLS, LA strain variables, and RVEF improved the discrimination and calibration of the model (Table S5).

To validate model performance, both 10-fold cross-validation and the validation cohort were used. The inclusion of RV strain in the baseline models, which were based on clinical and conventional imaging variables, improved model discrimination for both end points in both 10-fold cross-validation and the validation cohort (Table S6).

### Subgroup Analysis

T1 mapping data were available for 132 patients in the original development cohort and for all 273 patients in the validation cohort. Together, these patients constituted the subgroup with

T1 mapping data. The mean native T1 value and extracellular volume fraction in this subgroup were 1250.3 msec ± 125.0 and 29.7% ± 4.5, respectively (Table S7). RV GLS and RV GCS remained independent predictors of both end points in multivariable Cox regression analyses after separate adjustment for native T1 value and extracellular volume fraction (all models,  $P < .05$ ) (Tables 5 and S8).

### Reproducibility Analysis

Interobserver and intraobserver analyses indicated that all strain parameters derived from cardiac MRI FT had excellent reproducibility (all interclass and intraclass correlation coefficients > 0.85) (Table S9).

### Discussion

To the best of our knowledge, this is the first study to focus on the prognostic value of right ventricular (RV) dysfunction as evaluated with cardiac MRI feature tracking (FT) in a large cohort of patients with heart failure with preserved ejection fraction (HFpEF). Key insights include the following: RV global

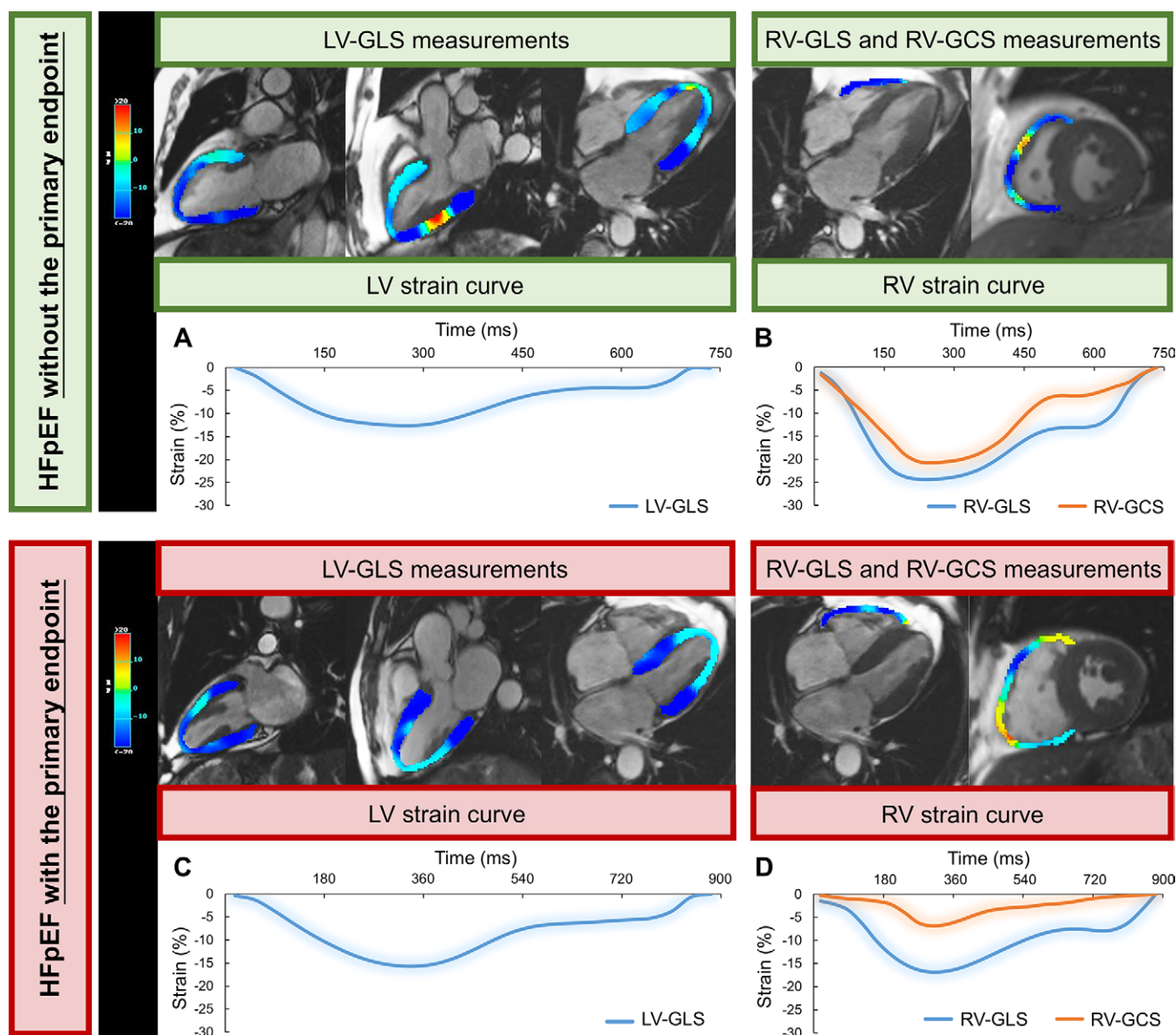


**Figure 3:** Representative cardiac MRI scans and plots of left ventricular (LV) and right ventricular (RV) strain measurements in two patients with heart failure with preserved ejection fraction (HFpEF): (A, B) a 70-year-old male patient who did not die and (C, D) a 67-year-old male patient who died during follow-up (primary end point). (A, C) Images in the two-, three-, and four-chamber views and LV global longitudinal strain (GLS) curve are shown. (B, D) Images in the four-chamber and short-axis views and RV GLS and RV global circumferential strain (GCS) curves are shown. The two patients had similar LV GLS values, yet the patient with impaired RV GLS and RV GCS died, whereas the patient with relatively preserved RV GLS and RV GCS did not die.

longitudinal strain (GLS) and RV global circumferential strain (GCS) derived from cardiac MRI FT were independently associated with all-cause mortality in patients with HFpEF (adjusted hazard ratio [HR] per 1% increase, 1.07 [ $P = .005$ ] and 1.13 [ $P < .001$ ], respectively). The incorporation of RV GLS and RV GCS into a predefined model based on clinical and conventional imaging variables or into a predefined model based on those variables plus left ventricular GLS improved model discrimination (C index, 0.794 vs 0.760 and 0.795 vs 0.771, respectively). RV GLS and RV GCS remained independent predictors after adjustment for tissue characterization parameters, including late gadolinium enhancement, native T1 value, and extracellular volume fraction (all models,  $P < .05$ ).

Several echocardiographic studies have highlighted the prognostic value of RV strain derived from speckle tracking in patients with HFpEF (12,13). For example, Hamada-Harimura et al (12)

prospectively studied 618 patients with acute decompensated HF, among whom 206 (33.3%) had HFpEF. In a subgroup analysis of patients with HFpEF, only impaired free wall RV GLS ( $\geq -13.1\%$ ; adjusted HR, 2.16;  $P = .01$ ) was independently associated with a composite end point of cardiovascular death and HF hospitalization. Another study focusing on patients with HFpEF reported that impaired RV GLS ( $> -17.5\%$ ) was an independent predictor of both a composite end point of all-cause death and HF hospitalization (adjusted HR, 2.10;  $P = .005$ ) and overall mortality (adjusted HR, 3.66;  $P = .001$ ) (13). Circumferential strain parameters derived from echocardiography have exhibited poor reproducibility, primarily due to the inferior image quality of short-axis views with this modality (24). Importantly, to our knowledge, previous echocardiographic studies have not evaluated the prognostic value of circumferential strain parameters. The present study focused on RV strain variables derived from cardiac MRI FT, which allow RV



**Table 3: Univariable and Multivariable Analysis for the Primary End Point**

Variable	Univariable Analysis		Multivariable Analysis*	
	Unadjusted HR	P Value	Adjusted HR	P Value
<b>Clinical variables</b>				
Age (per year)	1.07 (1.05, 1.09)	<.001	1.05 (1.03, 1.08)	<.001
Female sex	1.50 (1.01, 2.23)	.04		
Body mass index <sup>†</sup>	0.90 (0.85, 0.95)	<.001		
NYHA class III or IV	1.94 (1.25, 3.01)	.003		
Hypertension	1.45 (0.88, 2.38)	.15		
Coronary artery disease	1.45 (0.98, 2.14)	.06		
Diabetes	1.50 (1.00, 2.24)	.049		
Atrial fibrillation	1.22 (0.81, 1.83)	.34		
eGFR (mL/min/1.73 m <sup>2</sup> )	0.97 (0.96, 0.98)	<.001	0.99 (0.97, 1.00)	.009
NT-proBNP (pg/mL; log transformed)	3.37 (2.08, 5.48)	<.001		
<b>Conventional cardiac MRI variables</b>				
LV wall thickness (mm)	1.05 (1.00, 1.11)	.06		
LVEF (%)	0.95 (0.92, 0.99)	.006		
LVEDVi (mL/m <sup>2</sup> )	1.01 (1.00, 1.02)	.02		
LVESVi (mL/m <sup>2</sup> )	1.02 (1.01, 1.04)	.001		
LVMi (g/m <sup>2</sup> )	1.01 (1.00, 1.02)	.07		
LAEF (%)	0.98 (0.96, 0.99)	.001		
LAVi max (mL/m <sup>2</sup> )	1.01 (1.01, 1.02)	<.001	1.01 (1.00, 1.01)	.01
LAVi min (mL/m <sup>2</sup> )	1.02 (1.01, 1.02)	<.001		
RVEF (%)	0.98 (0.96, 0.99)	.01		
RVEDVi (mL/m <sup>2</sup> )	1.00 (0.99, 1.01)	.95		
RVESVi (mL/m <sup>2</sup> )	1.01 (1.00, 1.03)	.07		
Presence of LGE	2.19 (1.48, 3.22)	<.001	2.06 (1.40, 3.03)	<.001
Ischemic LGE	1.94 (1.28, 2.93)	.002		
Nonischemic LGE	1.70 (1.07, 2.68)	.02		
LGE mass (g)	1.02 (1.00, 1.04)	.03		
LGE percentage of LV mass (%)	1.03 (1.01, 1.05)	.009		
<b>Cardiac MRI–derived strain variables</b>				
LV GLS (%)	1.11 (1.05, 1.18)	<.001		
LV GCS (%)	1.09 (1.02, 1.16)	.006		
LV GRS (%)	0.96 (0.94, 0.99)	.007		
LA reservoir strain (%) <sup>‡</sup>	0.94 (0.92, 0.97)	<.001		
LA conduit strain (%) <sup>‡</sup>	0.91 (0.87, 0.95)	<.001		
LA booster strain (%) <sup>‡</sup>	0.94 (0.90, 0.98)	.002		
RV GLS (%)	1.10 (1.06, 1.15)	<.001	1.07 (1.02, 1.12)	.005
RV GCS (%)	1.16 (1.08, 1.24)	<.001	1.13 (1.05, 1.21)	<.001
RV GRS (%)	0.94 (0.91, 0.97)	<.001		

Note.—Data in parentheses are 95% CIs. Among the 1019 patients with heart failure with preserved ejection fraction, 103 died of any cause (primary end point). eGFR = estimated glomerular filtration rate, GCS = global circumferential strain, GLS = global longitudinal strain, GRS = global radial strain, HR = hazard ratio, LA = left atrium, LAEF = LA ejection fraction, LAVi max = LA maximum volume index, LAVi min = LA minimum volume index, LGE = late gadolinium enhancement, LV = left ventricle, LVEDVi = LV end-diastolic volume index, LVEF = LV ejection fraction, LVESVi = LV end-systolic volume index, LVMi = LV end-diastolic mass index, NT-proBNP = N-terminal fragment of the prohormone of brain natriuretic peptide, NYHA = New York Heart Association, RV = right ventricle, RVEDVi = RV end-diastolic volume index, RVEF = RV ejection fraction, RVESVi = RV end-systolic volume index.

\* Variables with  $P < .05$  in the univariable analysis were included in the multivariable analysis using a stepwise forward selection method. HRs are shown for variables that were independent predictors in the multivariable analysis.

<sup>†</sup> Calculated as weight in kilograms divided by height in meters squared.

<sup>‡</sup> LA reservoir, conduit, and booster strains were excluded from the multivariable analysis because more than 25% of the data were missing.

dysfunction to be used as a prognostic indicator in patients with HFpEF. Our results demonstrated that RV GLS and RV GCS were independently associated with adverse outcomes, and the incorporation of RV GLS and RV GCS into a model including clinical and conventional imaging variables improved model discrimination and calibration for these end points.

The RV chamber is adapted to low pulmonary resistance under normal conditions and is therefore highly sensitive to changes in afterload (7). RV strain is a sensitive marker for early or subclinical RV dysfunction, which is a critical sign of HF progression associated with an increased risk of mortality (3,5). We speculate that RV systolic function in patients with HFpEF



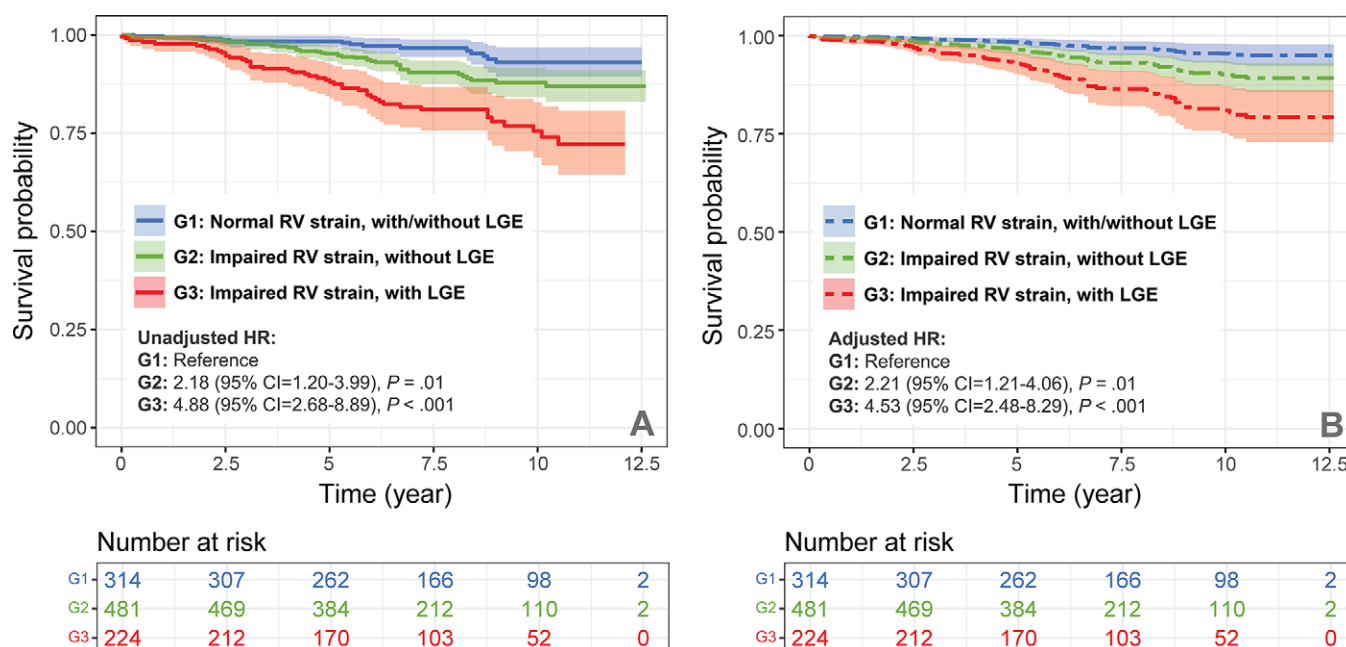


**Figure 4:** Comparison of time until all-cause death in patient groups with and without late gadolinium enhancement (LGE) and impaired right ventricular (RV) strain. Survival curves are shown for (A) the univariable analysis and (B) the multivariable analysis after adjustment for age, estimated glomerular filtration rate, and left atrial maximum volume index. Impaired RV strain was defined as RV global longitudinal strain or circumferential strain lower than their respective medians. Patients with impaired RV strain and LGE had poorer outcomes than those with normal RV strain, irrespective of the presence of LGE. G = group, HR = hazard ratio.

**Table 4: Incremental Prognostic Value of Cardiac MRI Metrics for the Primary End Point**

Model	Model Discrimination (Harrell C index)*	Model Calibration	
		$\chi^2$ Statistic	P Value
Model 1: clinical variables†	0.716 (0.661, 0.772)	63.37	Ref.
Model 2: model 1 + LAVi max	0.734 (0.681, 0.787)	78.53	.009
Model 3: model 2 + LGE	0.760 (0.712, 0.809)	93.99	<.001
Model 4: model 3 + RV strain‡	0.794 (0.750, 0.838)	126.90	<.001

Note.—LAVi max = left atrial maximum volume index, LGE = late gadolinium enhancement, Ref. = reference, RV = right ventricle.

\* Data in parentheses are 95% CIs.

† The clinical variables were age and estimated glomerular filtration rate.

‡ RV strain included RV global longitudinal and circumferential strain.

can reveal accommodation to the elevated afterload. The RV free wall is primarily composed of circumferential fibers; therefore, there is typically an elevation of RV GCS but a reduction in RV GLS in the compensatory phase of RV dysfunction (25,26). Hence, impaired RV GLS can serve as a more sensitive marker for detecting early RV dysfunction and predicting adverse events. During disease progression, RV GCS also decreases in the decompensated phase, and a lower value might be an indicator of progressed RV dysfunction, as evidenced by its higher HR for poor outcomes and greater relative importance in the full model than RV GLS. Importantly, the prognostic value of RV GLS and RV GCS was independent of LV parameters for tissue characterization, including late gadolinium enhancement, native T1 value, and extracellular volume fraction. Theoretically, changes in tissue characterization should precede changes in function (including strain). These findings

support the unique role of RV strain in prognostic evaluation, suggesting that it offers additional prognostic information beyond what is provided by conventional cardiac MRI tissue characterization.

In patients with HFpEF, conflicting results regarding the prognostic value of LV GLS have been reported across different echocardiographic (10,13) and cardiac MRI (11,17) studies; these discrepancies may be attributable to the complex etiology of HFpEF and the different inclusion and exclusion criteria of these studies. Due to the limited data on RV and LV strain variables in patients with HFpEF, whether RV strain variables provide superior prognostic value compared with LV GLS remains unclear. To date, only two studies involving RV and LV strain variables derived from speckle-tracking echocardiography have

shown that LV GLS was not associated with poor outcomes (12,13). Our study provides evidence from cardiac MRI FT in patients with less severe HFpEF (lower New York Heart Association class and lower incidence of mortality). In our study, both LV GLS and RV strain parameters derived from cardiac MRI FT were associated with adverse outcomes in the univariable analysis, but LV GLS was not an independent predictor in the multivariable analysis. This interesting finding suggests that the prognostic value of RV dysfunction in patients with HFpEF may surpass that of LV dysfunction. We hypothesize that in patients with HF, the prognostic value of RV dysfunction, which is a sign of HF progression, is independent of LV dysfunction. Furthermore, in patients with HFpEF, RV dysfunction may play a more important role in prognosis than LV dysfunction does because LV systolic function (ejection fraction) is relatively preserved in these patients.

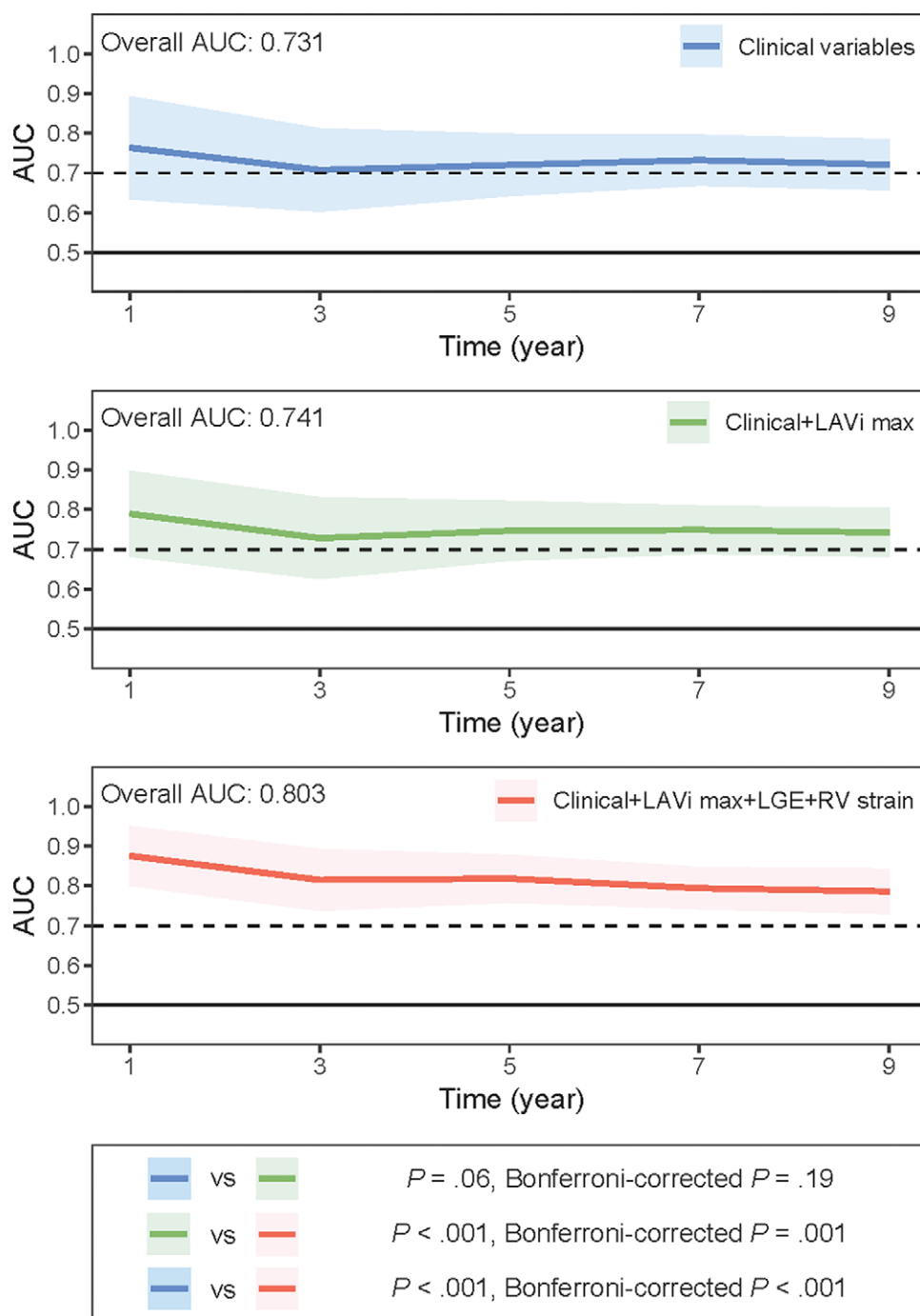


**Figure 5:** Time-dependent area under the receiver operating characteristic curve (AUC) for three prognostic models for all-cause death. The overall AUC represents the AUC for the entire follow-up period. *P* values were calculated using the DeLong test. The clinical variables were age and estimated glomerular filtration rate. The addition of late gadolinium enhancement (LGE) and right ventricular (RV) strain (global longitudinal and circumferential strain) to the baseline model significantly improved prediction accuracy. LAVi max = left atrial maximum volume index.

Our study had several limitations. First, this was a single-center retrospective study. Second, LA strain parameters were obtained in only 73% (745 of 1019) of patients because of atrial fibrillation during cardiac MRI examination. A study focusing on LA strain parameters derived from speckle-tracking echocardiography in patients with HFpEF was similarly affected (61% [307 of 505] of patients had LA strain parameters) (27). Third, our study involved scanners from multiple vendors with different field strengths (1.5 T and 3.0 T), which

could be a confounder (28). Finally, two limitations of the generalizability of our findings should be noted. The predominance of male patients (70%) in our cohort may limit the broader applicability of the results to other populations with a more balanced sex distribution. Also, the use of FT software from a single vendor for strain analysis may limit the generalizability of our findings to institutions using FT software from a different vendor, as variations between FT programs could contribute to heterogeneity in RV strain measurements (28).

**Table 5: Subgroup Analysis of Patients with T1 Mapping Data for the Primary End Point**

Variable	Hazard Ratio*	P Value
<b>Univariable analysis</b>		
Native T1 (per 10 msec)	1.04 (1.01, 1.07)	.007
ECV (%)	1.12 (1.03, 1.23)	.01
RV GLS (%)	1.14 (1.03, 1.26)	.01
RV GCS (%)	1.24 (1.04, 1.48)	.02
<b>Multivariable analysis</b>		
<b>Model S1</b>		
Native T1 (per 10 msec)	1.04 (1.01, 1.06)	.01
RV GLS (%)	1.13 (1.02, 1.27)	.03
<b>Model S2</b>		
Native T1 (per 10 msec)	1.04 (1.01, 1.07)	.009
RV GCS (%)	1.24 (1.04, 1.47)	.02
<b>Model S3</b>		
ECV (%)	1.13 (1.03, 1.24)	.01
RV GLS (%)	1.15 (1.03, 1.28)	.01
<b>Model S4</b>		
ECV (%)	1.11 (1.02, 1.22)	.02
RV GCS (%)	1.22 (1.03, 1.45)	.02

Note.—ECV = extracellular volume, GCS = global circumferential strain, GLS = global longitudinal strain, RV = right ventricle.

\* Unadjusted hazard ratio for univariable analysis; adjusted hazard ratio for multivariable analysis. Data in parentheses are 95% CIs.

In conclusion, right ventricular (RV) global longitudinal and circumferential strain derived from cardiac MRI feature tracking (FT) were independently associated with adverse outcomes in patients with heart failure with preserved ejection fraction (HFpEF). These findings offer novel insights into refining risk stratification in this patient population and provide evidence of the prognostic value of RV dysfunction as evaluated with cardiac MRI FT in patients with HFpEF. Future research should focus on prospective, large-scale, multicenter studies involving scanners and FT software from multiple vendors to further validate the potential of RV strain parameters for improving risk stratification in routine clinical settings. As we expand our understanding of HFpEF, there is an urgent need to consider biventricular function rather than focusing solely on left ventricular function in the management of HFpEF.

**Deputy Editor:** Rozemarijn Vliegthart

**Scientific Editor:** Shannyn Wolfe (AJE)

#### Author affiliations:

<sup>1</sup> Department of Magnetic Resonance Imaging, Fuwai Hospital, National Center for Cardiovascular Diseases, Chinese Academy of Medical Sciences and Peking Union Medical College, No 167 Beilishi Rd, Beijing 100037, China

<sup>2</sup> Department of Echocardiography, Fuwai Hospital, National Center for Cardiovascular Diseases, Chinese Academy of Medical Sciences and Peking Union Medical College, Beijing, China

<sup>3</sup> Key Laboratory of Cardiovascular Imaging (Cultivation), Chinese Academy of Medical Sciences, Beijing, China

<sup>4</sup> Department of Health and Human Services, National Heart, Lung, and Blood Institute, National Institutes of Health, Bethesda, Md

<sup>5</sup> Now with Division of Cardiovascular Medicine and Department of Radiology, University of Utah School of Medicine, Salt Lake City, Utah

<sup>6</sup> Oxford Centre for Clinical Magnetic Resonance Research, John Radcliffe Hospital, National Institute for Health Research Oxford Biomedical Research Centre, Oxford British Heart Foundation Centre of Research Excellence, University of Oxford, Oxford, United Kingdom

Received October 12, 2024; revision requested November 18; final revision received April 30, 2025; accepted May 2.

**Address correspondence to:** M.L. (email: coolkan@163.com).

**Funding:** This study was supported by the National Natural Science Foundation of China (grant no. 82471973), the Beijing Natural Science Foundation (grant no. 7242110), the Noncommunicable Chronic Diseases–National Science and Technology Major Project (grant no. 2023ZD0504502), the Chinese Academy of Medical Sciences Innovation Fund for Medical Sciences (grant no. 2021-I2M-1-063), and the Youth Key Program of High-Level Hospital Clinical Research (grant no. 2022-GSP-QZ-5).

**Acknowledgments:** The authors would like to thank Yang Wang, PhD, and Yanyan Zhao, PhD, from the Medical Research and Biometrics Center, National Center for Cardiovascular Diseases, Fuwai Hospital, and Enyu Tian, PhD, from the Department of Epidemiology, State Key Laboratory of Cardiovascular Disease, Fuwai Hospital, for their assistance with statistical analysis.

**Author contributions:** Guarantor of integrity of entire study, M.L.; study concepts/ study design or data acquisition or data analysis/interpretation, all authors; manuscript drafting or manuscript revision for important intellectual content, all authors; approval of final version of submitted manuscript, all authors; agrees to ensure any questions related to the work are appropriately resolved, all authors; literature research, L.Z., M.J., J.X., D.Z., W.Y., Y.W., A.E.A., S.Z., M.L.; clinical studies, L.Z., J.X., D.Z., W.W., Y.W., G.Y., M.L.; statistical analysis, L.Z., J.X., D.Z., M.L.; and manuscript editing, L.Z., J.X., W.Y., A.S., Q.Z., M.L.

**Disclosures of conflicts of interest:** L.Z. No relevant relationships. H.Z. No relevant relationships. M.J. No relevant relationships. J.X. No relevant relationships. D.Z. No relevant relationships. W.W. No relevant relationships. W.Y. No relevant relationships. Y.W. No relevant relationships. G.Y. No relevant relationships. A.S. No relevant relationships. A.E.A. Licensed software from Circle Cardiovascular Imaging. Q.Z. Grants or contracts from the British Heart Foundation. S.Z. No relevant relationships. M.L. No relevant relationships.

#### References

1. Tsao CW, Aday AW, Almarazooq ZI, et al; American Heart Association Council on Epidemiology and Prevention Statistics Committee and Stroke Statistics Subcommittee. Heart disease and stroke statistics—2023 update: a report from the American Heart Association. *Circulation* 2023;147(8):e93–e621.
2. Redfield MM, Borlaug BA. Heart failure with preserved ejection fraction: a review. *JAMA* 2023;329(10):827–838.
3. Melenovsky V, Hwang SJ, Lin G, Redfield MM, Borlaug BA. Right heart dysfunction in heart failure with preserved ejection fraction. *Eur Heart J* 2014;35(48):3452–3462.
4. Obokata M, Reddy YNV, Melenovsky V, Pislaru S, Borlaug BA. Deterioration in right ventricular structure and function over time in patients with heart failure and preserved ejection fraction. *Eur Heart J* 2019;40(8):689–697.
5. Mohammed SF, Hussain I, AbouEzzeddine OF, et al. Right ventricular function in heart failure with preserved ejection fraction: a community-based study. *Circulation* 2014;130(25):2310–2320.
6. Guazzi M, Ghio S, Adir Y. Pulmonary hypertension in HFpEF and HFrEF. *J Am Coll Cardiol* 2020;76(9):1102–1111.
7. Lang RM, Bierig M, Devereux RB, et al; European Association of Echocardiography. Recommendations for chamber quantification: a report from the American Society of Echocardiography's Guidelines and Standards Committee and the Chamber Quantification Writing Group, developed in conjunction with the European Association of Echocardiography, a branch of the European Society of Cardiology. *J Am Soc Echocardiogr* 2005;18(12):1440–1463.
8. Kraigher-Krainer E, Shah AM, Gupta DK, et al; PARAMOUNT Investigators. Impaired systolic function by strain imaging in heart failure with preserved ejection fraction. *J Am Coll Cardiol* 2014;63(5):447–456.
9. Xu J, Yang W, Zhao S, Lu M. State-of-the-art myocardial strain by CMR feature tracking: clinical applications and future perspectives. *Eur Radiol* 2022;32(8):5424–5435.
10. Shah AM, Claggett B, Sweitzer NK, et al. Prognostic importance of impaired systolic function in heart failure with preserved ejection fraction and the impact of spironolactone. *Circulation* 2015;132(5):402–414.
11. Kammerlander AA, Donà C, Nitsche C, et al. Feature tracking of global longitudinal strain by using cardiovascular MRI improves risk stratification in heart failure with preserved ejection fraction. *Radiology* 2020;296(2):290–298.

12. Hamada-Harimura Y, Seo Y, Ishizu T, et al; ICAS-HF Investigators. Incremental prognostic value of right ventricular strain in patients with acute decompensated heart failure. *Circ Cardiovasc Imaging* 2018;11(10):e007249.
13. Lejeune S, Roy C, Ciocea V, et al. Right ventricular global longitudinal strain and outcomes in heart failure with preserved ejection fraction. *J Am Soc Echocardiogr* 2020;33(8):973–984.e2.
14. Gorter TM, van Veldhuisen DJ, Bauersachs J, et al. Right heart dysfunction and failure in heart failure with preserved ejection fraction: mechanisms and management. Position statement on behalf of the Heart Failure Association of the European Society of Cardiology. *Eur J Heart Fail* 2018;20(1):16–37.
15. Ponikowski P, Voors AA, Anker SD, et al; ESC Scientific Document Group. 2016 ESC guidelines for the diagnosis and treatment of acute and chronic heart failure: the Task Force for the Diagnosis and Treatment of Acute and Chronic Heart Failure of the European Society of Cardiology (ESC) developed with the special contribution of the Heart Failure Association (HFA) of the ESC. *Eur Heart J* 2016;37(27):2129–2200.
16. Pieske B, Tschöpe C, de Boer RA, et al. How to diagnose heart failure with preserved ejection fraction: the HFA-PEFF diagnostic algorithm: a consensus recommendation from the Heart Failure Association (HFA) of the European Society of Cardiology (ESC). *Eur Heart J* 2019;40(40):3297–3317.
17. He J, Yang W, Wu W, et al. Early diastolic longitudinal strain rate at MRI and outcomes in heart failure with preserved ejection fraction. *Radiology* 2021;301(3):582–592.
18. Kramer CM, Barkhausen J, Bucciarelli-Ducci C, et al. Standardized cardiovascular magnetic resonance imaging (CMR) protocols: 2020 update. *J Cardiovasc Magn Reson* 2020;22(1):17.
19. He J, Sirajuddin A, Li S, et al. Heart failure with preserved ejection fraction in hypertension patients: a myocardial MR strain study. *J Magn Reson Imaging* 2021;53(2):527–539.
20. Voigt JU, Mălaescu GG, Haugaa K, Badano L. How to do LA strain. *Eur Heart J Cardiovasc Imaging* 2020;21(7):715–717.
21. Hicks KA, Tcheng JE, Bozkurt B, et al. 2014 ACC/AHA key data elements and definitions for cardiovascular endpoint events in clinical trials: a report of the American College of Cardiology/American Heart Association Task Force on Clinical Data Standards (Writing Committee to Develop Cardiovascular Endpoints Data Standards). *Circulation* 2015;132(4):302–361.
22. Lindholm D, Lindbäck J, Armstrong PW, et al. Biomarker-based risk model to predict cardiovascular mortality in patients with stable coronary disease. *J Am Coll Cardiol* 2017;70(7):813–826.
23. Zhao K, Zhu Y, Chen X, et al. Machine learning in hypertrophic cardiomyopathy: nonlinear model from clinical and CMR features predicting cardiovascular events. *JACC Cardiovasc Imaging* 2024;17(8):880–893.
24. Pedrizzetti G, Claus P, Kilner PJ, Nagel E. Principles of cardiovascular magnetic resonance feature tracking and echocardiographic speckle tracking for informed clinical use. *J Cardiovasc Magn Reson* 2016;18(1):51.
25. Bianco CM, Farjo PD, Ghaffar YA, Sengupta PP. Myocardial mechanics in patients with normal LVEF and diastolic dysfunction. *JACC Cardiovasc Imaging* 2020;13(1 Pt 2):258–271.
26. Tadic M, Pieske-Kraigher E, Cuspidi C, et al. Right ventricular strain in heart failure: clinical perspective. *Arch Cardiovasc Dis* 2017;110(10):562–571.
27. Kim D, Seo JH, Choi KH, et al. Prognostic implications of left atrial stiffness index in heart failure patients with preserved ejection fraction. *JACC Cardiovasc Imaging* 2023;16(4):435–445.
28. Yang W, Xu J, Zhu L, et al. Myocardial strain measurements derived from MR feature-tracking: influence of sex, age, field strength, and vendor. *JACC Cardiovasc Imaging* 2024;17(4):364–379.